J Mater Sci: Mater Med (2009) 20:271–279
DOI 10.1007/s10856-008-3567-2

Development of 3D PPF/DEF scaffolds using micro-stereolithography and surface modification

Phung Xuan Lan · Jin Woo Lee · Young-Joon Seol · Dong-Woo Cho

Received: 3 January 2008 / Accepted: 18 August 2008 / Published online: 3 September 2008
© Springer Science+Business Media, LLC 2008

Abstract Poly(propylene fumarate) (PPF) is an ultraviolet-curable and biodegradable polymer with potential applications for bone regeneration. In this study, we designed and fabricated three-dimensional (3D) porous scaffolds based on a PPF polymer network using micro-stereolithography (MSTL). The 3D scaffold was well fabricated with a highly interconnected porous structure and porosity of 65%. These results provide a new scaffold fabrication method for tissue engineering. Surface modification is a commonly used and effective method for improving the surface characteristics of biomaterials without altering their bulk properties that avoids the expense and long time associated with the development of new biomaterials. Therefore, we examined surface modification of 3D scaffolds by applying accelerated biomimetic apatite and arginine-glycine-aspartic acid (RGD) peptide coating to promote cell behavior. The apatite coating uniformly covered the scaffold surface after immersion for 24 h in 5-fold simulated body fluid (5SBF) and then the RGD peptide was applied. Finally, the coated 3D scaffolds were seeded with MC3T3-E1 pre-osteoblasts and their biologic properties were evaluated using an MTS assay and histologic staining. We found that 3D PPF/diethyl fumarate (DEF) scaffolds fabricated with MSTL and biomimetic apatite coating can be potentially used in bone tissue engineering.

P. X. Lan
Department of Mechanical Engineering, Hanoi University of Technology, 1A-Dai Co Viet Street, Hai Ba Trung District, Hanoi City, Vietnam

J. W. Lee · Y.-J. Seol · D.-W. Cho (✉)
Department of Mechanical Engineering, POSTECH, Pohang, Gyeongbuk 790-784, Republic of Korea
e-mail: dwcho@postech.ac.kr

1 Introduction

Tissue engineering is a field that offers great potential for regenerative medicine. The development of three-dimensional (3D) scaffolds that guide cells into forming functional engineered tissues is one of the most important areas of tissue engineering. Several techniques, including solvent casting, phase separation, gas foaming, and fiber bonding, have been used to fabricate porous polymer scaffolds for tissue engineering [1–3]. A common limitation of these fabrication techniques is the lack of precise control of the internal and external architecture of the scaffolds. Recently, moldless manufacturing techniques, known as solid free-form (SFF) techniques, have been successfully used to fabricate complex 3D scaffolds with controllable architecture using a number of materials, including polymers, ceramics, and composites [4–6]. Furthermore, when combined with clinical imaging data, these fabrication techniques may provide the ability to form constructs that are customized to the shape of the defect or injury. One such technique, micro-stereolithography (MSTL), has been developed to produce precise 3D microstructures layer by layer from functional materials, and biocompatible materials in particular [7]. This technique was developed from a stereolithography and the pore size, porosity, pore distribution, and shape of the scaffold can be controlled easily by adjusting the laser power, scan speed, and laser beam path [8]. MSTL also provides many benefits for fabricating 3D scaffolds over other SFF methods, such as fused deposition modeling (FDM), 3D printing, and selective laser sintering (SLS). MSTL allows the fabrication of complex 3D scaffolds with high resolution (500 nm) over a large range of pore sizes. It also does not require a high processing temperature in contrast to FDM and SLS [5]. In this study, we propose the use of 3D

porous scaffolds fabricated using MSTL to engineer bone tissue.

Poly(propylene fumarate) (PPF), an ultraviolet-curable and biodegradable polymer, possesses properties that are critical for its potential use for bone regeneration [9–12]. The first important property is the ease by which PPF can be degraded in vivo into its original fumaric acid and propylene glycol subunits, which are non-toxic in vivo. Second, PPF has excellent mechanical properties that are suitable for bone tissue engineering applications [9]. In addition, each subunit of PPF contains an activated unsaturated site that can be cross-linked with various agents, such as diethyl fumarate (DEF), methyl methacrylate, and N-vinylpyrrolidone, to improve its characteristics. There have been a number of studies of PPF synthesis, its properties, and applications [13]. However, most studies have focused on fabricating solid PPF for bone cement applications, whereas few studies have focused on using PPF as a material for porous scaffolds with controllable architecture [14]. The work presented here is one of the first reported attempts to design and fabricate porous PPF-based scaffolds using MSTL.

Surface properties play important roles in determining the initial responses of living cells to a biomaterial and then controlling cellular events, such as adhesion, proliferation, migration, and differentiation. However, it is difficult to develop a biomaterial with good bulk properties that also processes suitable surface properties for biomedical applications. For example, although poly(lactic-co-glycolic acid) (PLGA) seems to be biocompatible and suitable for tissue engineering, its mechanical strength and hydrophobic surface properties limit its use [15]. PPF-based materials are good candidates for bone regeneration both in vitro and in vivo because of their non-toxic biodegradable products, injectability, and excellent mechanical properties [9–12]. However, their surface properties, including hydrophobicity, are disadvantageous. Hence, surface modification of biomaterials with sufficient bulk properties, followed by special treatment to enhance the surface properties without changing the bulk properties, is a common and effective method to improve the performance and function of biomaterials while avoiding the high monetary and time investments associated with the development of new biomaterials.

As one of the primary components of the bone extracellular matrix (ECM), apatite has good characteristics for bone reconstruction [16]. However, its use as a bulk material in applications where high load or strain occurs is prevented by its poor mechanical properties. Therefore, coating of suitable substrates with apatite has attracted a great deal of attention in bone construction. To efficiently modify the internal pore wall surfaces without altering the bulk structure and properties of the scaffold, a biomimetic apatite coating method has been developed as a 3D surface modification to grow bonelike mineral in prefabricated porous polymer scaffolds using simulated body fluid (SBF) [15–18].

In some studies, substrates coated with ECM proteins such as fibronectin, collagen, or laminin, were shown to influence integrin expression, subsequently expediting cell adhesion, proliferation, and differentiation. However, the use of proteins has disadvantages, including undesirable immune responses and problems associated with protein denaturation [19]. These problems can be overcome by presenting cell recognition motifs as small immobilized peptides. The arginine-glycine-aspartic acid (RGD) peptide sequence in many ECM proteins serves as a cell attachment cue; thus, coating with RGD peptides is an effective method of surface modification. RGD-coated substrates have been reported to increase cell spreading, proliferation, and differentiation in vitro [20, 21].

In this study, biomimetic apatite coating and RGD coating were examined in 3D PPF porous scaffolds to determine their ability to promote cell behavior, including cell attachment and proliferation. This is one of the first attempts to apply biomimetic surface modification to 3D porous PPF/DEF scaffolds for bone tissue engineering. In addition to demonstrating the clinical applications of this technology, we carried out a cell culture experiment with MC3T3-E1 pre-osteoblasts on the 3D scaffolds. MTS assay and histologic staining were used to evaluate the effects of surface coating on the 3D PPF/DEF scaffolds with MC3T3-E1 pre-osteoblasts.

2 Materials and methods

2.1 Synthesis of PPF

Poly(propylene fumarate) was synthesized by a condensation reaction according to the method of Gerhart et al. [9] with the following modifications; 2.4 mol of fumaric acid (278.40 g powder) and 3 mol of propylene glycol (228.18 g liquid) were placed in a triple-neck 1,000 ml flask with an overhead electrical stirrer, a thermometer, and a Barrett trap beneath a condenser. During synthesis, the mixture was stirred continuously at about 150 rpm. The mixture was maintained at 140°C for 16–17 h, during which time about 45 ml of water was collected. Then, the temperature was increased to 185–190°C to remove the excess propylene glycol and low molecular weight impurities. After 4–5 h at this temperature, the reaction was terminated. The product was kept at room temperature overnight to prevent further polymerization. Figure 1 shows the PPF synthesis process.

The molecular weight of the PPF polymer was estimated using a gel permeation chromatography (GPC) system with

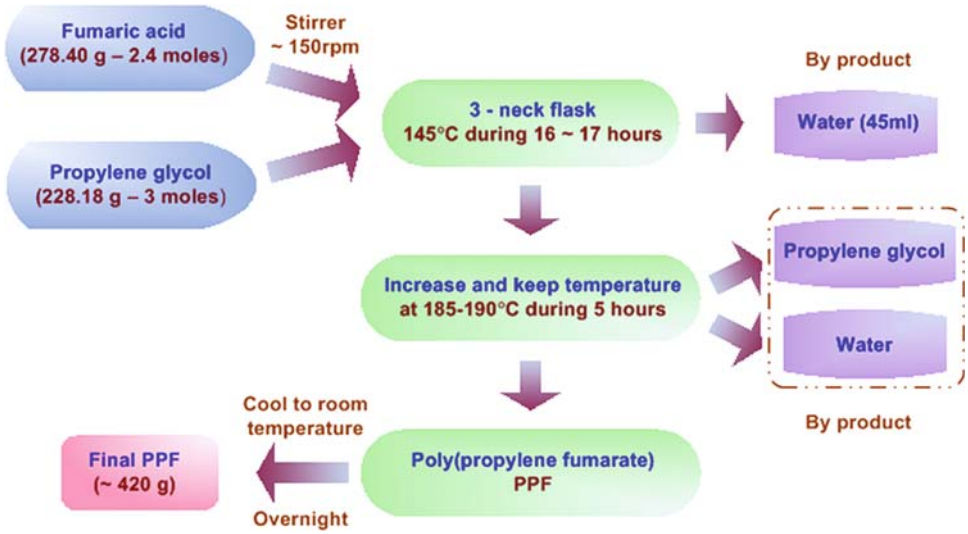

Fig. 1 PPF synthesis process

an ultraviolet detector at 260 nm. Samples were eluted with $CHCl_3$ through a Styrogel column at a flow rate of 1 ml/min. Molecular weight was determined relative to a polystyrene standard by the data plotting. The PPF polymer had Mn = 310, Mw = 1,307, and PDI = 4.22. The mechanical properties of synthesized PPF/DEF are similar to those of trabecular bone [11].

The PPF polymer has high viscosity at room temperature. To be able to use PPF as a resin for the MSTL system, DEF was added at a ratio of 70:30 to reduce the viscosity. First, the PPF was heated to approximately 60°C to decrease its viscosity and DEF was added. After mixing for about 1 h, the PPF/DEF mixture was filtered to remove impurities. Finally, the photoinitiator bis-acyl phosphine oxide (BAPO) was added at 1% (wt/wt) and the final mixture was stirred continuously for 3–4 h. The final mixture was filtered once more before use. A hot plate was controlled at the working temperature of 30°C.

2.2 Scaffold design and fabrication

In our MSTL system, a continuous-wave Ar ion laser with a wavelength of $\lambda = 351.1$ nm (Spectra-Physics BeamLok 2065-4S; Newport Corp., Irvine, CA, USA) was used as the light source. The laser was focused on the polymer surface and the stage was moved along the x-, y-, and z-axes to determine the position for solidification. A schematic diagram of the MSTL system is shown in Fig. 2. The photopolymer was processed in layers under laser irradiation to form 3D structures as a physical representation of a computer-aided design (CAD) model [22]. A hot plate was used at a working temperature of about 30°C to decrease the viscosity of the PPF/DEF mixture.

The 3D scaffold was computationally designed with alternating lattices and columns. Figure 3(a) and (b) show the overlapping lattice design and a 3D view of the scaffold design, respectively. The lattice and column layers were

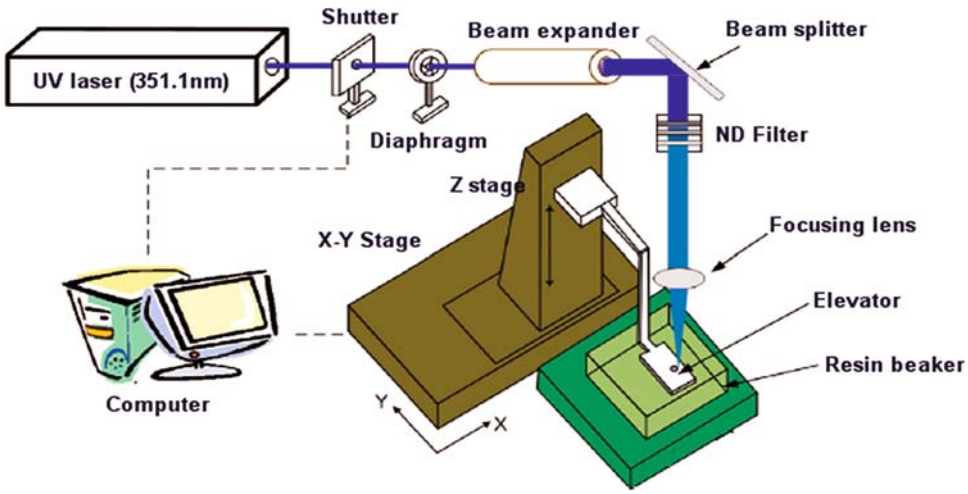

Fig. 2 Schematic diagram of the micro-stereolithography system

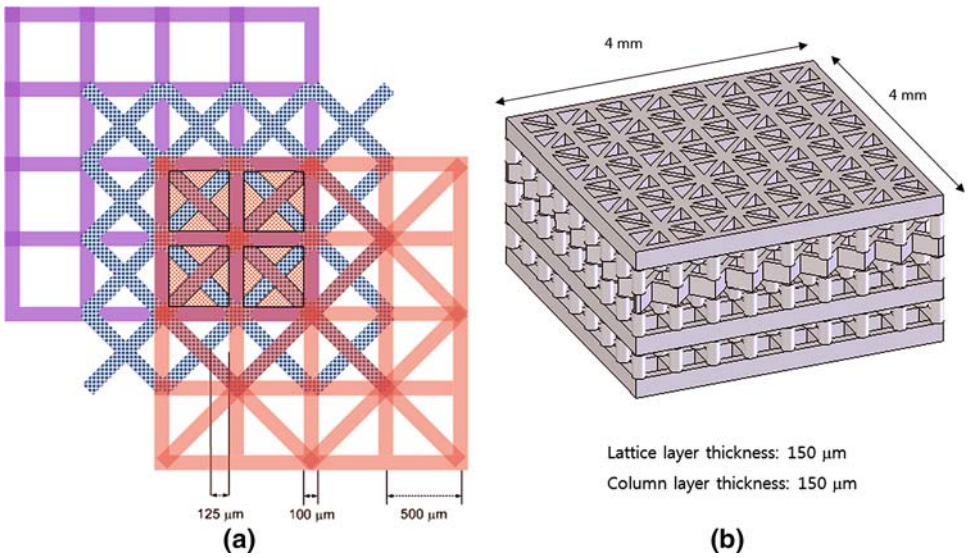

Fig. 3 3D scaffold designs: Overlapping lattice design (**a**) and 3D view (**b**)

each 150 μm thick. As three columns were stacked, the final column height was 450 μm. Thirteen layers were stacked, giving a final scaffold height of 1.95 mm. A 3D PPF/DEF scaffold was fabricated successfully using the MSTL system at a scan speed of 60 mm/min and a laser power of 350 μW. After fabrication, the structure was cleaned overnight using hot isopropanol (IPA) and ultrasound. A post-curing time of 10 h was required before further use.

2.3 Surface modification

Before modifying the scaffolds, they were sterilized for 1 h in 70% ethanol, washed for 1 h in phosphate-buffered saline (PBS), and dried.

For biomimetic apatite coating, the scaffold was immersed in fivefold SBF (5SBF) containing almost five times the inorganic ion concentration of human blood plasma. This solution was prepared by dissolving NaCl, $NaHCO_3$, KCl, $K_2HPO_4 \cdot 3H_2O$, $MgCl_2 \cdot 6H_2O$, $CaCl_2$, and Na_2SO_4 in distilled deionized water. The reagents used to prepare 200 ml of 5SBF are shown in Table 1. The pH of the solution was adjusted to 6.7 at 36.5°C with 1 M HCl and Tris.

A PPF/DEF plate measuring ϕ 9 × 0.5 mm was immersed in 20 ml of 5SBF in a plastic bottle at 37°C. After 24 h, the specimen was removed and washed carefully with distilled deionized water and dried in air. Three 3-D PPF/DEF scaffolds were immersed for 24 h in 20 ml of 5SBF with stirring at 37°C. The scaffolds were removed and rinsed twice with PBS. Sterilized filter paper was used to gently absorb most of the water from porous specimens. The scaffolds were dried in a clean bench at room temperature.

For biomimetic apatite and RGD coating, the 3D PPF/DEF scaffolds were first coated with apatite and then immersed in 10 ml of peptide solution (100 μg/ml RGD peptide in PBS) for 12 h in an incubator. Then, the scaffolds were removed, washed, and dried as described above.

Table 1 Order of addition and amounts of reagents used to prepare 200 ml of 5SBF

Order	Reagent	Amount
1	NaCl	8.035 g
2	$NaHCO_3$	0.355 g
3	KCl	0.225 g
4	$K_2HPO_4 \cdot 3H_2O$	0.231 g
5	$MgCl_2 \cdot 6H_2O$	0.311 g
6	1.0 M HCl	20 ml
7	$CaCl_2$	0.292 g
8	Na_2SO_4	0.072 g
9	Tris	2.060 g
10	1.0 M HCl	0–1 ml

2.4 Cell isolation and culture

The MC3T3-E1 pre-osteoblasts were a gift from Kyungpook National University Hospital, Taegu, South Korea. The digest was strained through a cell strainer (Falcon, Franklin Lakes, NJ, USA) and centrifuged at 1,000 rpm for 5 min to isolate the MC3T3-E1 pre-osteoblasts. The isolated pre-osteoblasts were plated on ϕ 100 tissue culture plates and incubated in 10 ml of α-minimal essential medium (MEM) containing 10% fetal bovine serum (Gibco, Grand Island, NY, USA), 100 units of penicillin/ml, and 100 μg of streptomycin/ml (Gibco). The medium was changed 2–3 days after seeding and the attached cells were then cultured. These MC3T3-E1 pre-osteoblasts were used in this study.

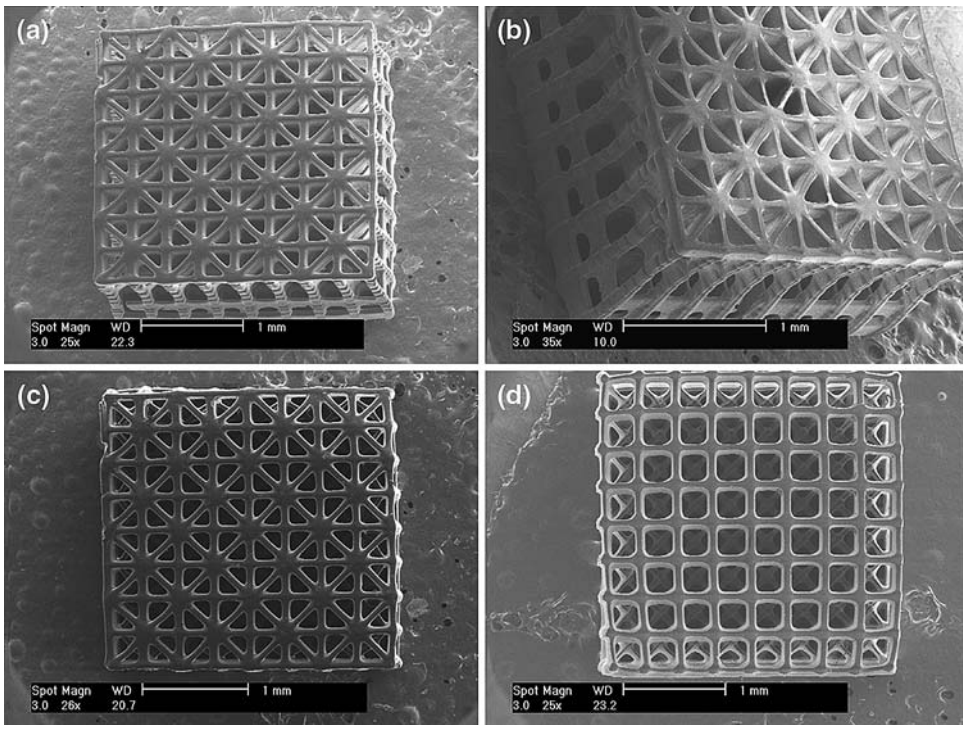

Fig. 4 3D Scaffold fabrication results: 3D view (**a**, **b**), top view (**c**), and bottom view (**d**)

MC3T3-E1 cells (10^5) were suspended in 10 μl of medium and the cell suspensions were pipetted onto scaffolds. The cells were allowed to adhere to the scaffolds for 1 h. Then, 700 μl of medium was added to each well of a 24-well plate (BD Falcon, Boston, MA, USA). Culture medium was changed every 2–3 days.

2.5 MTS assay

The mitochondrial metabolic activity of the cells was determined by MTS assay. Briefly, the scaffolds were rinsed in PBS, and then 240 μl of MTS (3-(4,5-dimethylthiazol-2-yl)-5-(3-carbonxylmethoxyphenyl)-2-(4-sulfophenyl)-2H-tetrazolium) was added to each well. After incubation for 6 h, the MTS solution was removed, and the optical density was measured at 490 nm using a plate reader.

2.6 Histologic staining

To evaluate the morphology of MC3T3-E1 pre-osteoblasts attached to the scaffolds, histologic images were taken after 2 weeks in culture. The cells attached to the scaffolds were fixed with 10% formalin for 1–2 h. The fixed cells on scaffolds were stained with hematoxylin and eosin (H&E) in situ, embedded in Tissue-Tek OCT compound (Miles Scientific, Naperville, IL, USA) and sectioned at a thickness of 10 μm. Photographs were taken of scaffold sections using a microscope.

3 Results

3.1 Scaffold fabrication

Figure 4 shows the 3D scaffold fabrication results. The scaffold was well fabricated with a line width of 90 μm, pore size of 250 μm, and top surface of 110 μm. Due to the overlapping lattice design, the pores extending from the top to the bottom of the scaffold were 75 μm in diameter. The porosity of the scaffold was 65%, calculated using data measured after fabrication. Since all of the pores were interconnected in the scaffold design, scaffold pore interconnectivity was 100%. Compared to the design, 25% shrinkage was observed post-curing. Although scaffolds did shrink post-curing, the shrinkage directions of the scaffold were isotropic. Therefore, we can predict and compensate for the degree of shrinkage. The majority of the shrinkage effect can be solved using a compensatory structure fabrication code, which was generated by the databases accumulated from preliminary experiments. In the case of more precise shapes and parts, we can fabricate structures by fine-tuning the compensatory code.

3.2 Apatite characterization

The PPF/DEF plates and scaffolds were incubated in 5SBF at 37°C for 24 h. Scanning electron microscopy (SEM) images of the PPF/DEF plates before and after incubation are shown in Fig. 5. The untreated PPF/DEF surface was

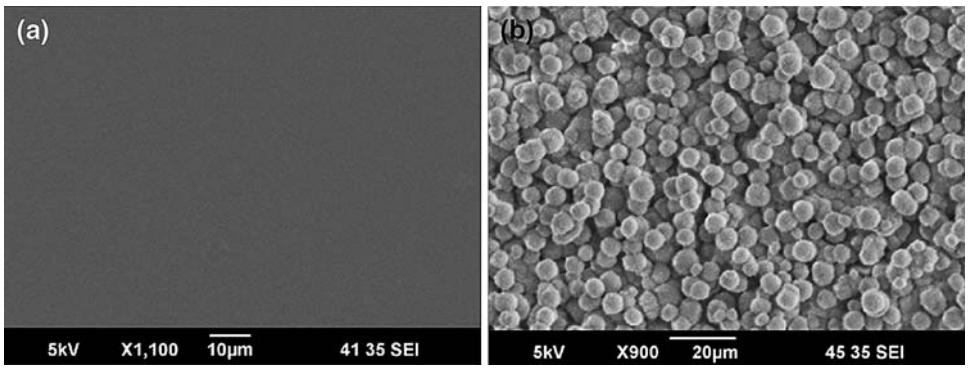

Fig. 5 SEM images of PPF/DEF plates incubated in 5SBF for 0 h (**a**) and 24 h (**b**)

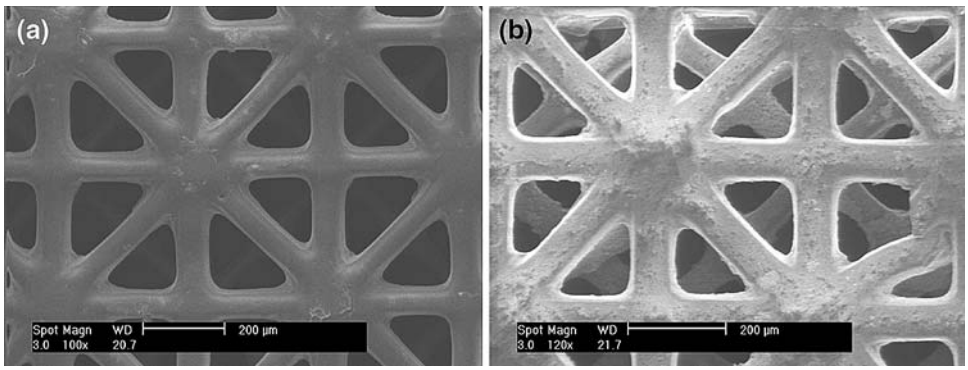

Fig. 6 SEM images of PPF/DEF scaffolds incubated in 5SBF for 0 h (**a**) and 24 h (**b**)

very smooth (Fig. 5 (a)), whereas the modified surface covered with apatite micro-particles was rough (Fig. 5 (b)).

Figure 6 shows SEM images of PPF/DEF scaffolds before and after incubation in 5SBF for 24 h. The apatite micro-particles were uniformly deposited on the surface of the PPF/DEF scaffolds. The aggregation of these micro-particles formed a thin film on the scaffold surface. More apatite micro-particles were observed at the intersection of the line structure.

3.3 X-ray diffraction

X-ray diffraction (XRD) spectra were obtained with an X-ray diffractometer with a fixed incidence of 1° in the range of 15–40° using steps of 0.06° and 1 s/step scan speed. The XRD patterns of PPF/DEF plates before and after incubation in 5SBF for 24 h are shown in Fig. 7. The characteristic peaks of PPF/DEF without coating are shown in pattern A. Coated PPF/DEF plates also had characteristic peaks (31.56–31.88°C) corresponding to the (211) plane of apatite, as shown in pattern B.

3.4 MTS assay

MC3T3-E1 pre-osteoblasts were cultured on scaffolds to evaluate cell behavior and the effects of surface coating. Scaffolds were immersed in the cultures for 1 day, 1 week, or 2 weeks. The results of MTS assay of the effects of biomimetic apatite coating on MC3T3-E1 pre-osteoblast growth are shown in Fig. 8. Cells increased in number with culture time, both with and without the coating. From the MST assay results, cell adhesion results of 1 day after cell seeing did not tell the superiority among each conditions. However, cell proliferation results of apatite and apatite-RGD-coated scaffold were better than that of a control scaffold after 1 week and 2 weeks. These cell culture results indicate that biomimetic apatite coating can modify the surface of PPF/DEF scaffolds and promote cell proliferation.

3.5 Histologic staining

Examination of longitudinal sections of scaffolds showed that cells adhered to and proliferated very well on the inner architecture of scaffolds with apatite coating and apatite-RGD coating. In contrast, not many cells were observed in control scaffolds. The results shown in Fig. 9 also indicate that the biomimetic apatite coating and apatite-RGD coating influenced cell proliferation. However, it was difficult to tell whether the apatite or the apatite-RGD coating was better from the H&E staining results.

4 Discussion

This study was performed to develop 3D PPF/DEF scaffolds using the MSTL system for bone tissue engineering

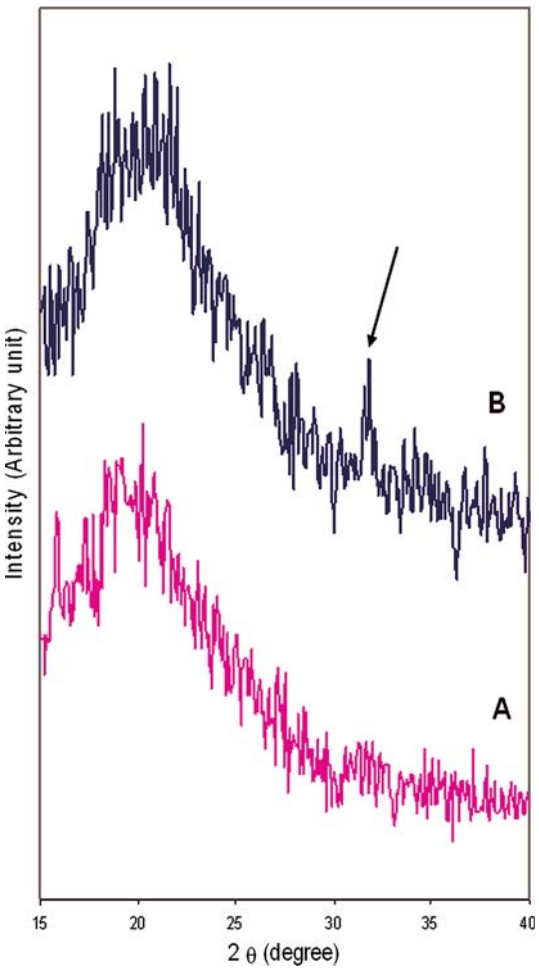

Fig. 7 X-ray diffraction patterns of (**a**) PPF/DEF plate without coating and (**b**) PPF/DEF plate with apatite coating (the arrow indicates the characteristic peak of apatite)

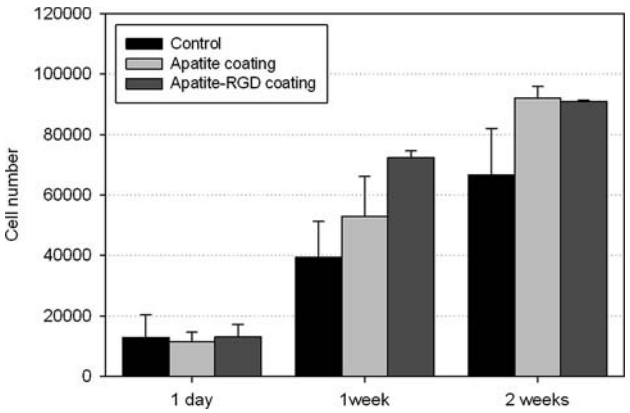

Fig. 8 Effects of biomimetic apatite and RGD coating on MC3T3-E1 pre-osteoblast growth

applications, and to determine the effects of surface modifications, including biomimetic apatite and RGD coatings, on 3D PPF/DEF scaffolds in terms of cell attachment and proliferation. We investigated a novel application of PPF-based materials, in MSTL systems as a 3D porous scaffold material. The PPF/DEF polymer was synthesized according to the method of Gerhart et al. [10], with modifications to make it suitable for the MSTL system in terms of solidification. 3D PPF/DEF scaffolds were fabricated successfully with uniform line width and pore size, as well as high porosity.

Using MSTL technology, we can fabricate the scaffold from defect information (e.g., bone defect and loss) obtained from medical data (e.g., CT, MRI images) of patients. Therefore, this method can provide custom-made scaffolds for patients. This is a noteworthy merit compared to conventional scaffold fabrication methods, such as salt leaching. MSTL technology also has merits in fabricating the inner architecture, as well as custom-made outer shapes. This technology allows us to control pore architectures, including the pore shape and size, thereby removing the uncertainty associated with pore irregularity. Therefore, we can standardize scaffolds and eliminate experimental errors due to irregular scaffolds in comparative experiments. Further, by controlling the inner architecture, our scaffold system will supply a perfectly interconnected inner structure, which can transport nutrients and exhaust wastes without any accumulation of media. The rates of cell proliferation and tissue regeneration inside the scaffold will be greater than those observed from conventional methods. Scaffolds that possess perfect interconnectivity do not need very high porosity for sufficient metabolism. Therefore, this benefit can preserve the preferred mechanical properties together with inner architecture design of the scaffold, which can sustain a high load.

The cell culture results, indicating that cell number increased with culture time, confirmed that this scaffold design supports cell proliferation and that PPF-based materials are biocompatible. Although shrinkage (calculated at 25%) can be a significant problem, we found that this shrinkage was isotropic in length and uniform in batches of several hundred scaffolds. Thus, shrinkage can be controlled and compensated for to obtain complex 3D scaffolds with the desired dimensions. However, further experiments are required to obtain precise structures.

The biomimetic apatite coating method used here has been applied to many substrates, including PLGA and polycaprolactone (PCL), and can significantly promote cell behavior [15–17], but there have been few studies of biomimetic apatite coating on 3D PPF/DEF scaffolds. SEM and XRD confirmed that the apatite coating was uniformly generated on the PPF/DEF surface and also on the scaffold after 24 h in 5SBF. This is a simple and effective method for apatite coating onto 3D scaffolds without any specialized equipment. The MTS assay results, as shown in the 1-day incubation results in Fig. 8, suggest that surface coating did not enhance MC3T3-E1 pre-osteoblast

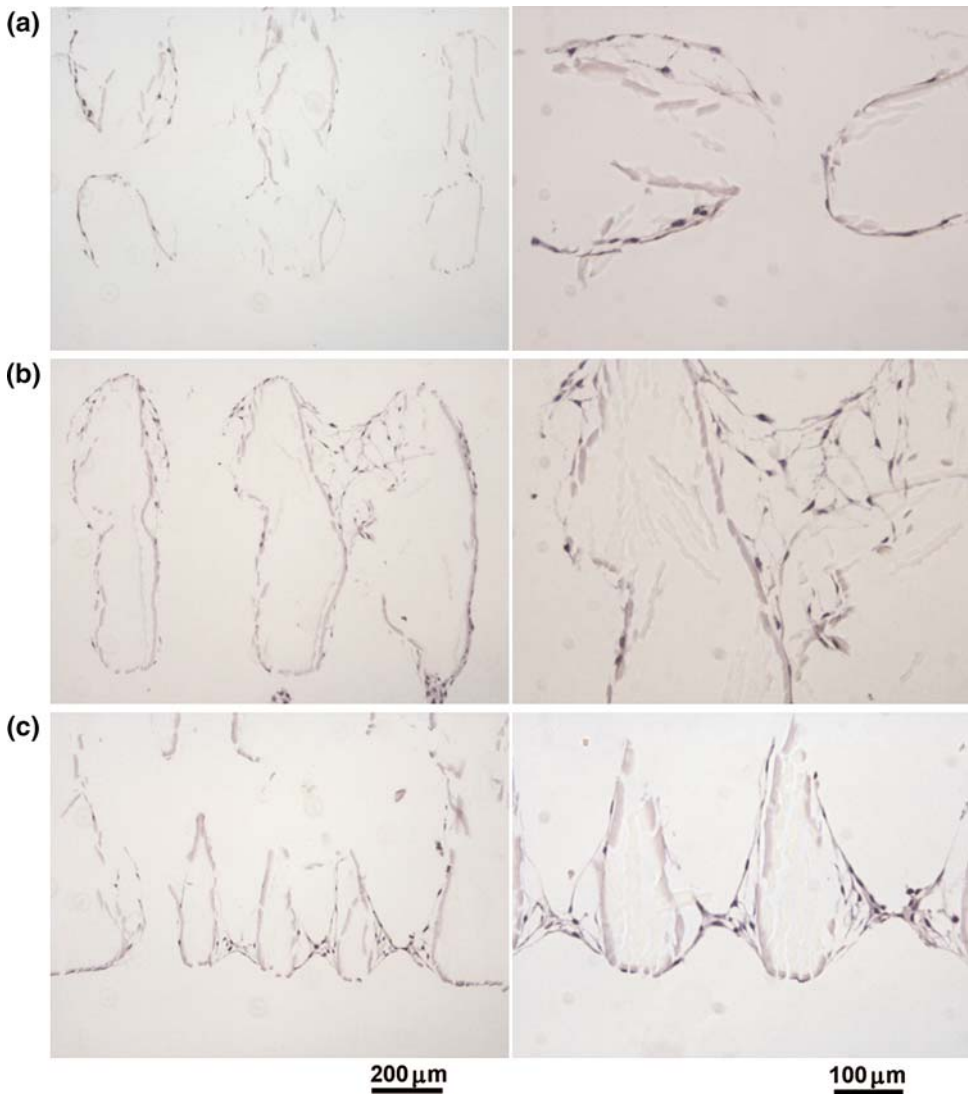

Fig. 9 Histologic staining (with H&E) of 3D PPF/DEF scaffolds after 2 weeks in culture for (**a**) control, (**b**) apatite coating, and (**c**) apatite-RGD coating, (left 100×, right 200×)

adhesion in the early stages. Based on the cell proliferation seen in both control and coated scaffolds, we demonstrated the biocompatibility of both the PPF/DEF material and the surface coating. A significant difference in cell number was observed after 1 week between control and apatite-coated scaffolds, and cell number was even higher after 2 weeks. The cell adhesion results for surface-coated scaffolds after 1 day of incubation could be improved if the apatite-coated scaffold was carefully rinsed, and if inorganic particles and weakly bound apatite micro-particles on the surface of the scaffold were completely removed. In addition, the surface of a pure PPF/DEF substrate was so smooth that the adhesion of apatite was markedly reduced. To resolve this problem, some studies used an acid or alkali pre-treatment to increase surface roughness as well as the apatite bond strength [23]. Despite this problem, the MTS assay results still demonstrated substantial effects of apatite coating on cell proliferation.

The histologic staining results agreed with the MTS results. The pre-osteoblasts strongly attached to the surface of scaffold columns and were in contact with each other. PPF/DEF scaffolds with apatite or apatite-RGD coating were more suitable for pre-osteoblast adhesion and proliferation. This may be attributable to the biocompatibility of the apatite coating and also the surface roughness resulting from the coating. Our results were in agreement with those of previous studies of biomimetic apatite coating on other substrates. However, the additional RGD coating did not provide additional benefits beyond those of the apatite coating.

5 Conclusions

In this study, we investigated a novel biomaterial for use as a bone tissue engineering construct. This material, based on

a biodegradable PPF polymer network, was successfully synthesized by radical reaction of PPF and DEF at a ratio of 70:30.

3D PPF/DEF scaffolds were fabricated using MSTL with controllable architecture features, such as shape, pore size, and porosity. These features can be controlled easily by changing the laser power, scan speed, and laser beam path used. These results indicate that MSTL is a promising method for scaffold fabrication applied to bone tissue engineering.

In addition, we found good responses of MC3T3-E1 pre-osteoblasts to 3D PPF/DEF scaffolds, especially for cell proliferation. An apatite layer was successfully formed on PPF/DEF plates and 3D scaffolds within 24 h by an accelerated biomimetic process (5SBF). In addition to saving time, this coating method can be applied easily to 3D scaffolds without altering the bulk structure or properties of the scaffolds. We also showed that MC3T3 pre-osteoblast compatibility with PPF/DEF scaffolds was greatly enhanced with biomimetic apatite coating, whereas RGD coating after apatite coating did not further enhance pre-osteoblast attachment or proliferation.

In conclusion, 3D PPF/DEF scaffolds fabricated by MSTL with accelerated biomimetic apatite coating can potentially be applied to bone tissue engineering to enhance cell proliferation.

Acknowledgments This work was supported by the Korea Science and Engineering Foundation (KOSEF) through the National R&D Project (M10646020003–06N4602–00310), the National Research Laboratory Program (R0A–2005–000–10042–0(2007)), and National R&D Project for Nano Science and Technology (M10203000020–07M0300–02010) funded by the Ministry of Science and Technology.

References

1. P.X. Ma, Mater. Today **7**, 30 (2004). doi:10.1016/S1369-7021(04)00233-0
2. D.W. Hutmacher, Biomaterials **21**, 2529 (2000). doi:10.1016/S0142-9612(00)00121-6
3. A.J. Salgado, O.P. Coutinho, R.L. Reis, Macromol. Biosci. **4**, 743 (2004). doi:10.1002/mabi.200400026
4. S.J. Hollister, Nat. Mater. **4**, 518 (2005). doi:10.1038/nmat1421
5. K.F. Leong, C.M. Cheah, C.K. Chua, Biomaterials **24**, 2363 (2003). doi:10.1016/S0142-9612(03)00030-9
6. D.W. Hutmacher, M. Sittinger, M.V. Risbud, Trends Biotechnol. **22**, 353 (2004). doi:10.1016/j.tibtech.2004.05.005
7. J.W. Lee, P.X. Lan, B. Kim, G. Lim, D.W.B. Cho, Microelectron. Eng. **84**, 1702 (2007). doi:10.1016/j.mee.2007.01.267
8. J.-H. Sim, E.-D. Lee, H.-J. Kweon, IJPEM **8**, 50 (2007)
9. A.J. Domb, United States Patent 4888413 (1989)
10. D.D. Frazier, V.K. Lathi, T.N. Gerhart, W.C. Hayles, J. Biomed. Mater. Res. **35**, 383 (1997). doi:10.1002/(SICI)1097-4636(19970605)35:3<383::AID-JBM12>3.0.CO;2-G
11. J.P. Fisher, D. Dean, A.G. Mikos, Biomaterials **23**, 4333 (2002). doi:10.1016/S0142-9612(02)00178-3
12. J.P. Fisher, J.W.M. Vehof, D. Dean, J.P.C.M. Van Der Waerden, T.A. Holland, A.G. Mikos et al., J. Biomed. Mater. Res. **59**, 547 (2002). doi:10.1002/jbm.1268
13. S.J. Peter, M.J. Miller, M.J. Yaszemski, A.G. Mikos, in *Handbook of Biodegradable Polymers*, ed. by A.J. Domb, J. Kost, D.M. Wiseman (Harwood Academic Publishers, Newark, 1997), p. 87
14. M.N. Cooke, J.P. Fisher, D. Dean, C. Rimnac, A.G. Mikos, J. Biomed. Mater. Res. Part B Appl. Biomater. **64B**, 65 (2002). doi:10.1002/jbm.b.10485
15. R. Zhang, P.X. Ma, Macromol. Biosci. **4**, 100 (2004). doi:10.1002/mabi.200300017
16. R. Murugan, S. Ramakrishna, Compos. Sci. Technol. **65**, 2385 (2005). doi:10.1016/j.compscitech.2005.07.022
17. T. Kokubo, H. Takadama, Biomaterials **27**, 2907 (2006). doi:10.1016/j.biomaterials.2006.01.017
18. Y. Chen, A.F.T. Mak, J. Li, M. Wang, A.W.T. Shum, J. Biomed. Mater. Res. Part B Appl. Biomater. **73B**, 68 (2005). doi:10.1002/jbm.b.30178
19. Y. Chen, A.F.T. Mak, M. Wang, J. Li, M.S. Wong, Surf. Coat. Technol. **201**, 575 (2006). doi:10.1016/j.surfcoat.2005.12.005
20. U. Hersel, C. Dahmen, H. Kessler, Biomaterials **24**, 4385 (2003). doi:10.1016/S0142-9612(03)00343-0
21. A.A. Sawyer, K.M. Hemmessy, S.L. Bellis, Biomaterials **26**, 1467 (2005). doi:10.1016/j.biomaterials.2004.05.008
22. I.H. Lee, D.W. Cho, Int. J. Adv. Manuf. Technol. **22**, 410 (2003). doi:10.1007/s00170-003-1538-9
23. T. Miyazaki, H.-M. Kim, T. Kokubo, J. Mater. Sci.: Mater. Med. **12**, 683 (2001). doi:10.1023/A:1011260224120